

**MID-INFRARED REFLECTANCE SPECTROSCOPY OF SHOCK ANALOGS FOR THE BEPICOLOMBO**

**MISSION** Aleksandra N. Stojic<sup>1</sup>, Andreas Morlok<sup>1</sup>, Peter Tollan<sup>2,5</sup>, Tomas Kohout<sup>3</sup>, Juulia Moreau<sup>3</sup>, Iris Weber<sup>1</sup>, Harald Hiesinger<sup>1</sup>, Jörg Hermann<sup>2</sup>, Maximilian P. Reitze<sup>1</sup>, Karin E. Bauch<sup>1</sup>, Joern Helbert<sup>4</sup> <sup>1</sup>Institut für Planetologie, Wilhelm-Klemm-Strasse 10, 48149, Germany; <sup>2</sup>Institut für Geologie, Baltzerstrasse 1+3, 3012 Bern, Switzerland; <sup>3</sup>Department of Geosciences and Geography, P.O. Box 64, 00014 Helsinki, Finland; <sup>4</sup>Institute for Planetary Research, DLR, Rutherfordstrasse 2, 12489 Berlin, Germany; <sup>5</sup>Institute of Geochemistry and Petrology, Clausiusstr. 25, 8092 Zürich, Switzerland. A.stojic@uni-muenster.de

**Introduction:** BepiColombo is the joint ESA/JAXA space mission to Mercury. Launched in October 2018, “Bepi” will reach its science mapping orbit in 2026 [1]. MERTIS, the Mercury Radiometer and Thermal Infrared Spectrometer, is part of the scientific payload and will provide spectral information in the range between 7  $\mu\text{m}$  – 14  $\mu\text{m}$  of Mercury’s surface [2].

In order to deconvolute the MERTIS infrared data, laboratory spectra for comparison are needed. A wide range of natural mineral and rock samples, such as impact rocks and meteorites were investigated spectrally [e.g. 3, 4]. However, since meteorites originating from Mercury have not been discovered yet, spectra of analog material that best represent the mineral constituents of Mercury’s crust have been included into the database, currently being built at the Westfälische - Wilhelms Universität Münster. Space weathering (SW) [5] might be affecting Mercury’s crust strongly. As micrometeorite bombardment is a significant SW agent, our experiments aim at documenting mineral specific shock load responses spectrally.

San Carlos olivine ( $\sim\text{Fo}_{87}$ ) particulates that experienced shock load were investigated optically and spectrally in order to account for shock-induced changes that might alter un-shocked olivine spectral signatures, focusing on mineral diagnostic spectral characteristics, e.g., Christiansen feature (CF) and Reststrahlen bands (RBs), data which were previously lacking in the database.

Two diagnostic areas, a ‘melt patch’ (red outline, Fig. 1a), where melting and cooling features were observed and adjacent fractured crystalline material (yellow outline, Fig. 1b) are presented in this work.

**Samples and Techniques:** *Sample Production:* We crushed San Carlos ( $\sim\text{Fo}_{87}$ ) single crystals in an agate mortar for approximately 1 h. The obtained powder was not sieved ( $< 380 \mu\text{m}$ ) and we did not compress the mineral powder in order to preserve the pore space enclosed by particulates. The porosity was estimated to  $\sim 40\%$  using the simple relation between sample weight, density and volume of the sample chamber.

*Shock recovery experiment:* The powder was placed into an indentation (25 mm x 2 mm) of the smaller of two ARMCO - Fe cylinders ( $\text{Ø} = 30 \text{ mm}$ ), the bigger cylinder ( $\text{Ø} \sim 50 \text{ mm}$ ) enclosed the smaller assemblage

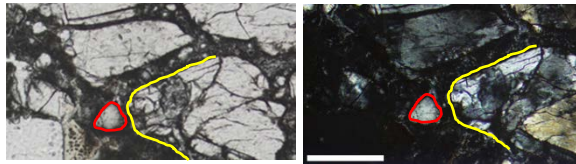
containing the sample and in this way sealed off the olivine sample safely. Both cylinders were set into a steel sleeve that serves as a momentum trap. A 4 mm thick steel flyer plate is accelerated with explosives towards the ARMCO Fe/sample/steel assemblage. The experimental assembly is depicted and described in Fig. 1 in [6]. Calculated shock wave reverberations lead to peak shock pressures of approximately 33 GPa. However, uncompressed powder is not in full contact with the sample chamber walls, which is required in order to calculate impedances at interfaces correctly and due to enclosed air locally drastically different values are expected. However, observed undulose extinction, planar fractures and mosaicism are indicative of peak pressures up to 30 GPa [7]. The peak T can be inferred from the  $\text{Fo}_{87}$  melting point at 1890 C. The pressure and local post-shock temperature rise led to a heterogeneous distribution of shock signatures throughout the sample portion as described in the following paragraphs.

**Electron probe micro analyzer (EPMA):** We obtained backscatter electron (BSE) images of several selected areas of the polished thin section to document melting and cooling patterns (Fig. 2 a and b) with a JEOL JXA-8530F. The probe was operated at an excitation voltage of 15 kV and a beam current of 15 nA.

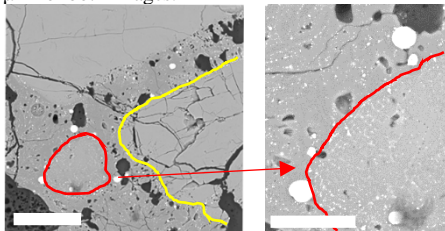
**Infrared Spectroscopy: Reflectance** FTIR maps of a thin section (24  $\mu\text{m}$  thick) produced from the shocked sample were generated with a Bruker Hyperion 3000 equipped with a focal plane array (FPA) mapping detector combined with a 15x Cassegrain objective at the University of Bern. The native resolution of the FPA detector is  $\sim 2.7 \mu\text{m}$  (4096 spectra distributed evenly over a fixed 170 x 170  $\mu\text{m}$  measurement area). In order to improve spectral quality, 4 adjacent pixels were combined (binned) to produce a final resolution of  $\sim 5.4 \mu\text{m}$ . Multiple mapping grids were distributed over the target areas of the thin section. Areas of interest were identified on the thin section and single spectra were extracted using the OPUS software. The spectral intensity of selected areas was normalized according to minimum and maximum intensity in the range between  $1150 \text{ cm}^{-1}$  –  $850 \text{ cm}^{-1}$  to better compare the rise or decline of specific RBs within a certain orientation. As all analyses were obtained from single selected grains or re-worked interstitial areas the spectra obtained from grain fragments resemble specular reflectance measurements.

**Results & Discussion:** We identified distinct “interaction areas” that hint at different P, T – conditions within the sample material optically using a petrographic microscope and an EPMA – namely: (1) heavily to intermediate fractured grains (e.g., yellow outline, Fig. 1 a), (2) melt patches with typical cooling patterns (EPMA BSE, Fig. 2 a - b) and (3) undulose extinguishing grains on the verge of mosaicism throughout the entire thin section. A change in RB position or intensity and/or reflectance minima within the resulting olivine spectra (see Figs. 3 and 4) is mainly attributed to orientation effects of the measured single crystals [8,9].

**Conclusions:** Although we observe classic shock patterns in the entire thin section optically and have evidence of melt formation in some areas, the corresponding spectra show rather unperturbed silicate features in the MIR range. A very robust RB of olivine is located at  $\sim 980 \text{ cm}^{-1}$  and could probably serve as a “proxy” for olivine in mineral mixtures.



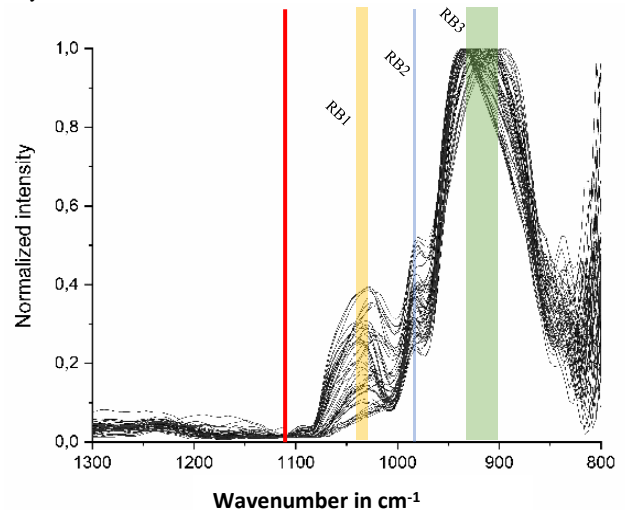
**Figs. 1 a - b:** a) and b) petrographic image of reworked area (ra) A) parallel nicols – image shows dark interstitial matter (finest fraction + residual resin), fractured crystal fragments (yellow outline) and melt patch (red outline in both images). B) crossed nicols image shows bright melt patch (red outline) and bright crystal fragments. Interstitial material remains dark under crossed nicols. Scale bar (white) is 100  $\mu\text{m}$  for both images.



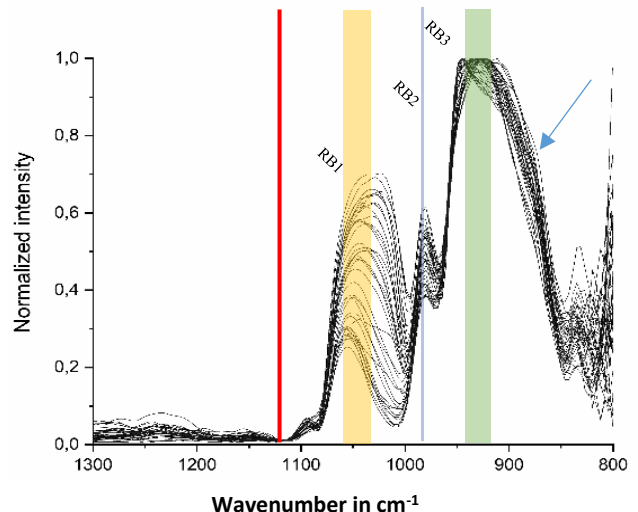
**Figs. 2 a - b:** EPMA - BSE micrograph of area depicted in Figs. 1 a - b. a) Red outline shows cooling patterns of two immiscible liquids (Fe-metal and silicate melt), yellow enclosed area is a heavily fragmented adjacent olivine grain b) Higher magnification image of red outline in 1 a); Bright Fe-rich patterns set within a darker silicate matrix show a typical graphic texture. Spectra from red outlined area are shown in Fig. 3, spectra from yellow outline in Fig. 4. Scale bar is 40  $\mu\text{m}$  in both images.

**Acknowledgments:** Financial support provided by DLR grant 50 QW 1302/1701 in the framework of the BepiColombo mission (A.M., I.W., A.N.S., M.P.R., K.B.) We thank Profs. Alexander Deutsch and Kai Wünnemann for advice on the shock experiment, Michael Feldhaus for production of the sample containers and Ulla Heitmann for careful handling of the recovered samples. Many thanks to Prof. Anne Hofmeister for valuable information on orientation effects in olivine single crystals.

**References:** [1] Benkhoff J. et al. (2010) Planetary and Space Science 58, 2-20 [2] Hiesinger H. et al. (2010) PSS 58, 144-165 [3] Morlok et al. (2020) Icarus 335, 113410 [4] Weber I. et al. (2020) Earth and Planetary Science Letters 530, 115884 [5] Domingue D. et al. (2014) Space Science Rev 181, 121-214 [6] Müller et al. (1969) EPSL 7, 251 - 264 [7] Stöffler et al. MAPS, 53(1), 5-49. [8] Reynard B. (1991) Phys Chem Minerals 18, 19-25 [9] Hofmeister A. (1987) Phys Chem Minerals 14, 499-513.



**Figs. 3:** Min/max normalized spectra extracted from the red outlined area (melt patch) in Figs. 1 & 2. Depicted are 58 spot measurements. The CF is located at  $1117 \text{ cm}^{-1}$  (red line). Mean values for the strongest RBs and their respective standard deviation (sd) are RB1 at  $1030 \text{ cm}^{-1}$  (sd = 6; orange shaded area), RB2 at  $982 \text{ cm}^{-1}$  (sd = 2; blue shaded area), and RB3 at  $907 \text{ cm}^{-1}$  (sd = 13; green shaded area). Note that RB1 is in some spectra completely absent, probably due to newly crystallized minute olivine crystals, cracks, melt or larger metal fractions.



**Figs. 4:** Min/max normalized spectra extracted from the yellow outlined area in Figs. 1 & 2. Depicted are 42 spot measurements. The CF is located at  $1117 \text{ cm}^{-1}$ . Mean values for the strongest RBs and their respective standard deviation (sd) are RB1 at  $1043 \text{ cm}^{-1}$  (sd = 10; orange shaded area), RB2 at  $981 \text{ cm}^{-1}$  (sd = 2; blue shaded area), and RB3 at  $931 \text{ cm}^{-1}$  (sd = 11; green shaded area). Note that RB3 has an additional shoulder (blue arrow) in 26 out of 42 spectra.